J. Biomed. Eng. Res.
Vol.26, No.3, 171-176, 2005

Automatic Liver Segmentation of a Contrast Enhanced CT Image Using an Improved Partial Histogram Threshold Algorithm

Kyung-Sik Seo[1], Seung-Jin Park[2]

[1] Electrical & Computer Engineering, New Mexico State University, Las Cruces, USA.
[2] Dept. of Biomedical Engineering, College of Medicine, Chonnam National University, Gwangju, Korea.

(Received June 7, 2004. Accepted March 30, 2005)

Abstract: This paper proposes an automatic liver segmentation method using improved partial histogram threshold (PHT) algorithms. This method removes neighboring abdominal organs regardless of random pixel variation of contrast enhanced CT images. Adaptive multi-modal threshold is first performed to extract a region of interest (ROI). A left PHT (LPHT) algorithm is processed to remove the pancreas, spleen, and left kidney. Then a right PHT (RPHT) algorithm is performed for eliminating the right kidney from the ROI. Finally, binary morphological filtering is processed for removing of unnecessary objects and smoothing of the ROI boundary. Ten CT slices of six patients (60 slices) were selected to evaluate the proposed method. As evaluation measures, an average normalized area and area error rate were used. From the experimental results, the proposed automatic liver segmentation method has strong similarity performance as the MSM by medical Doctor.

Key words: Computed Tomography, Partial histogram threshold, Binary morphological filtering

INTRODUCTION

Computed tomography (CT) is currently a conventional and excellent tool for diagnosis of the liver in medical imaging technology. The CT provides the detailed image and characteristics of a tumor and cancer for resection and transplantation of the liver. Periodical monitoring of CT images after treatment and cure helps a patient obtain full recovery from the cancer. If CT images are analyzed for early detection of liver tumor, treatment and curing may be easy and human life can be prolonged. The first significant process for liver diagnosis of the CT image is to segment the liver structure from other abdominal organs.

Liver segmentation using the CT image has been performed very often to diagnose liver disease.

Bae et al [1] used priori information about liver morphology and image processing techniques such as gray-level thresholding, Gaussian smoothing, mathematical morphology techniques, and B-splines. Gao et al [2] developed automatic liver segmentation using a global histogram, morphologic operations, and the parametrically deformable contour model. Tsai [3] proposed an alternative segmentation method using an artificial neural network to classify each pixel into three categories. Also, Husain et al [4] used neural networks for feature based recognition of liver region. In order to overcome semi-automatic liver segmentation [1-4], fully automatic liver segmentation was proposed [5,6]. However, proposed fully automatic liver segmentation has been problems with neighboring abdominal organs such as spleen, pancreas, and kidneys.

In this paper, an automatic liver segmentation method using an improved partial histogram threshold (PHT) algorithms is proposed to remove neighboring abdominal organs. In the following section, liver segmentation using improved PHT algorithms is presented. then experiments and their results are demonstrated. Finally, the conclusion will be given in the last section.

Corresponding Author: Seung-Jin Park, 8 Hak-dong, Dong-gu, Gwangju, 501-757, South Korea Dept. of Biomedical Engineering, Chonnam National University Hospital.
Tel. 062-220-6070, Fax. 062-226-4762
E-mail. sjinpark@jnu.ac.kr

LIVER SEGMENTATION

In this section, liver segmentation using improved PHT algorithms is presented. An adaptive

multi-modal threshold (AMT) method is first performed to find a region of interest (ROI) of the liver structure. A left partial histogram threshold algorithm removes other abdominal organs from the ROI. A right PHT (RPHT) algorithm removes the right kidney. Then, binary morphological (BM) filtering is processed for removing of small unnecessary objects and smoothing of the boundary. Liver segmentation is described in the block diagram of Fig. 1.

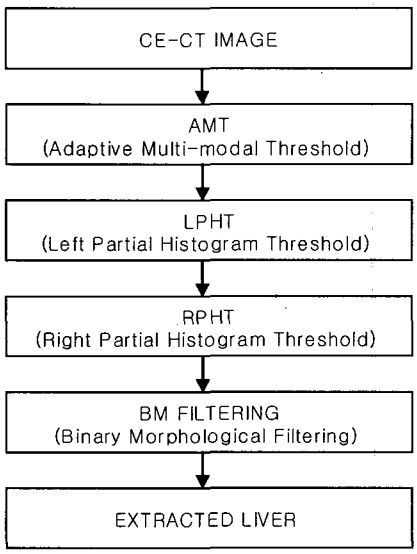

Fig. 1. The overall block diagram of the proposed liver segmentation algorithms.

Adaptive Multi-Modal (AMT) Threshold

An adaptive multi-modal threshold (AMT) method is used to extract the ROI. The AMT method is processed regardless of histogram variation derived from the contrast enhancement. Let Z^2 be an image domain and Z be a histogram domain. Let $I: Z^2 \rightarrow Z$ be a gray-level CE-CT image and (m, n) be a pixel location. Then, $I(m, n): Z^2 \rightarrow Z$. Also, the histogram, $h(k): Z \rightarrow Z$, is defined as [7]

$$h(k) = \{(m, n) \mid I(m, n) = k\} \quad (1)$$

where k is a gray-level value.

In order to remove histogram noise, the histogram is transformed by convolution and scaling [8]. Then the range of background and extremely enhanced organs such as bones and vessels is removed. After finding a global peak in the multi-modal histogram, the left and right valleys are calculated using a piecewise linear interpolation (PLI) method [9].

Each valley is found at the turning point from a negative value to a positive value because each point represents the slope. Left and right valleys become one range of an object. Then, the extracted range is removed from the transformed histogram h_t and this process is repeated until several ranges are found. The important range in this research is the range including the ROI of the liver. Regardless of any liver slice, pixel values of the ROI are located experimentally in the right side of the histogram because of pixel enhancement of CE-CT images. Let $[k_1, k_2]$ be the extracted lower and upper threshold integer values containing pixels of the ROI. Then $ROI: Z^2 \rightarrow Z^2$ is defined as

$$ROI = \{(m, n) \mid k_1 \leq I(m, n) \leq k_2\} \quad (2)$$

Fig. 2 shows the example of the AMT method. Fig. 2(a) is a gray-level CT image obtained from contrast media and Fig. 2(b) is a transformed histogram h_t using convolution and scaling. Fig. 2(c) and 2(d) are the ROI's range and ROI obtained by the AMT method. Also, Fig. 2(e) displays the ROI which includes kidneys and spleen after unnecessary small objects are removed.

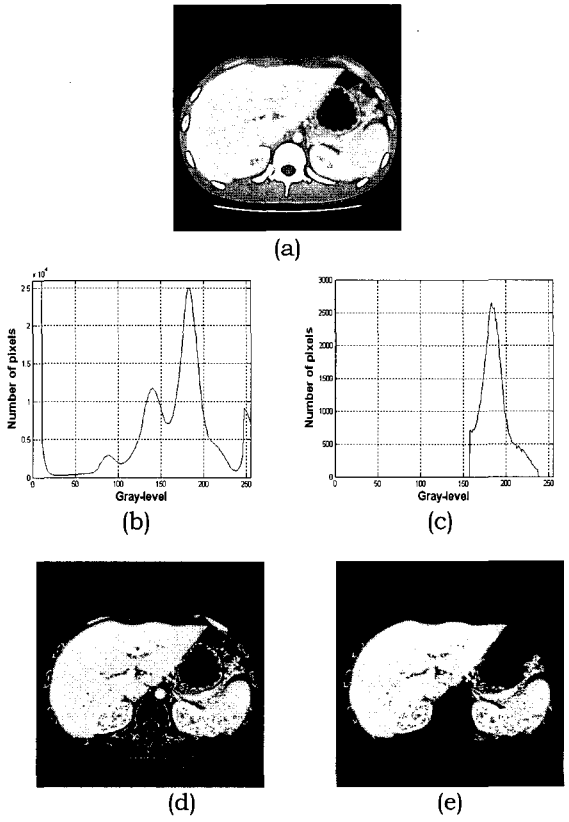

Fig. 2. AMT (Adaptive Multi-modal Threshold): (a) gray-level CT image, (b) transformed histogram (c) range of ROI after AMT, (d) ROI after AMT, and (e) ROI after small objects are removed.

Left Partial Histogram Threshold (LPHT) Algorithm

If the ROI has similar pixel values with other organs such as the pancreas, spleen, and left kidney, liver segmentation from ROI has a serious problem. Using higher contrast enhancement of the liver than the pancreas and spleen, a LPHT algorithm is proposed to solve this problem.

Let $h_{ROI}(k_1, k_2): Z \rightarrow Z$ be the histogram of ROI with the range $[k_1, k_2]$. Let I_{LPHT} be the LPHT image. Then the LPHT algorithm is proposed as shown in Fig. 3.

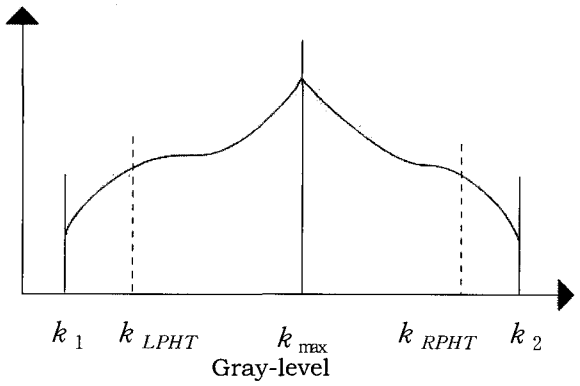

Fig. 3. Detailed histogram $h_{ROI}(k_1, k_2)$ for PHT algorithms.

- Find k_{max} where k_{max} is the gray-level value when $h_{ROI}(k)$ is the maximum value.
- Calculate left partial histogram interval $\Delta_{LPH} = (k_{max} - k_1)$.
- Find the left partial histogram threshold value $k_{LPHT} = (k_{max} - \Delta_{LPH}/2)$.
- Create the LPHT image I_{LPHT} defined as $I_{LPHT} = \{(m, n) \mid k_1 \le ROI(m, n) \le k_{LPHT}\}$.

After obtaining I_{LPHT} by the LPHT algorithm, ROI_{diff} is calculated from $I_{ROI} - I_{LPHT}$. Then neighboring abdominal organs such as the pancreas, spleen, and left kidney are removed from ROI_{diff} using area and location estimation [6].

Fig. 4(a) and 4(b) show the thresholded left partial histogram and LPHT image I_{LPHT} created by the LPHT algorithm. Fig. 4(c) and 4(d) show ROI_{diff} and the gray-level image ROI_{LPHT} which includes the right kidney after removing other abdominal organs.

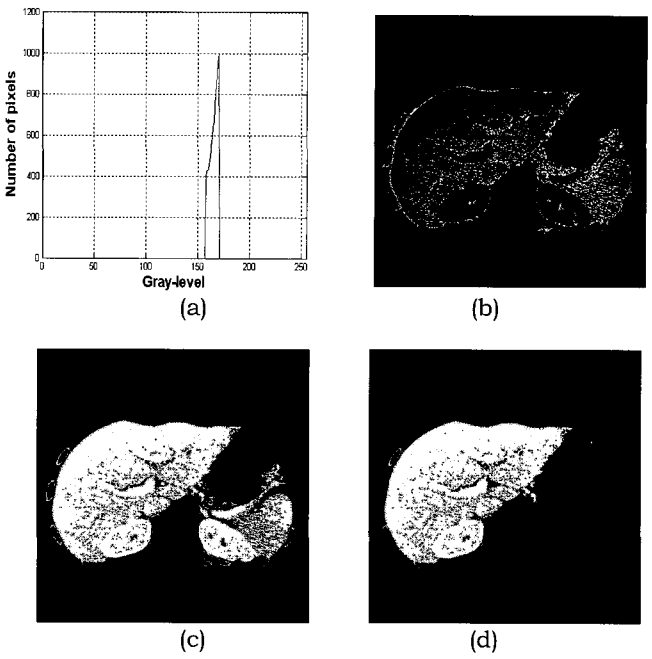

Fig. 4. Left partial histogram threshold (LPHT): (a) thresholded left partial histogram, (b) LPHT image I_{LPHT}, (c) different image ROI_{diff}, and (d) gray-level image of ROI_{LPHT} after removing other abdominal organs.

Right Partial Histogram Threshold (RPHT) Algorithm

A right partial histogram threshold (RPHT) algorithm is performed to remove the right kidney using less contrast enhancement of the liver than the kidney. The right kidney with an elliptic shape is neighbored with the lower liver part. However, this kidney creates a problem to segment a liver structure because of same gray-level values as liver vessels.

Let $h_{ROI}(k_1, k_2): Z \rightarrow Z$ be the histogram of ROI_{LPHT} with the range $[k_1, k_2]$. Let I_{RPHT} be the RPHT image. Then the RPHT algorithm is proposed as shown in Fig. 3:

- Find k_{max} where k_{max} is the gray-level value when $h_{ROI}(k)$ is the maximum value.
- Calculate right partial histogram interval $\Delta_{RPH} = (k_2 - k_{max})$.
- Find the right partial histogram threshold value $k_{RPHT} = (k_{max} + \Delta_{RPH}/8)$.
- Create the RPHT image I_{RPHT} defined as $I_{RPHT} = \{(m, n) \mid k_{RPHT} \le ROI_{LPHT}(m, n) \le 255\}$.

After obtaining I_{RPHT} by the RPHT algorithm, the right kidney image I_{kidney} is extracted from I_{RPHT} using area and angle estimation [6]. Then the gray-level image ROI_{RPHT} is calculated from $ROI_{LPHT} - I_{kidney}$.

Fig. 5(a) and 5(b) show the thresholded left partial histogram and RPHT image I_{RPHT} created by the RPHT algorithm. Fig. 5(c) shows the extracted right kidney I_{kidney} using area and angle estimation. Also, Fig. 5(d) shows the gray-level image ROI_{RPHT}.

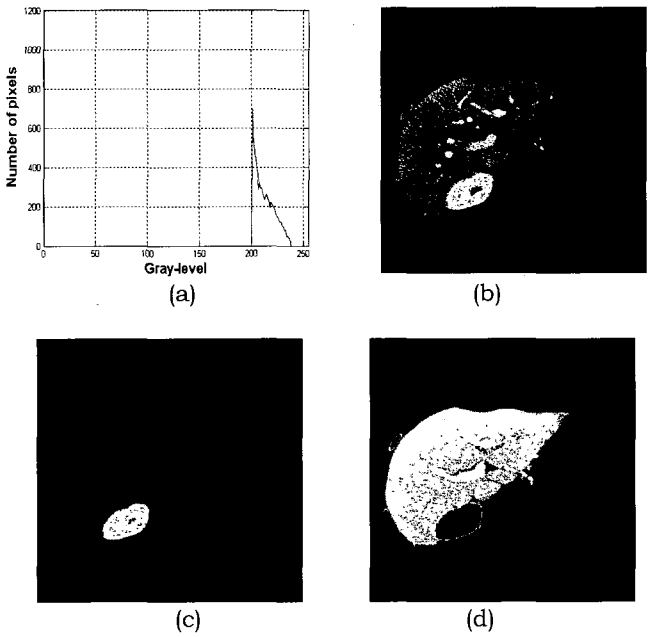

Fig. 5. Right partial histogram threshold (RPHT): (a) thresholded right partial histogram, (b) RPHT image I_{RPHT}, (c) extracted right kidney I_{kidney}, and (d) gray-level image ROI_{RPHT}.

Binary Morphological (BM) Filtering

BM filtering is processed to remove unnecessary small objects and to smooth the liver boundary. The gray-level image ROI_{RPHT} is transformed to the binary image, B, is defined as

$$B=\begin{cases} 1 & \text{if } k_1 \le ROI_{RPHT}(m,n) \le k_2 \\ 0 & \text{if } otherwise \end{cases} \quad (3)$$

where k_1 and k_2 are the gray-level range of ROI_{RPHT}.. As a SE is the spatial mask, the 8-connected SE is used in this research. Let $SE_2 \subset Z^2$ be a 2 by 2 matrix whose elements are 1 and $SE_3 \subset Z^2$ be a 3 by 3 matrix whose elements are 1.

Basically used BM filtering is dilation and erosion [10, 11]. Let $D^i(B): Z^2 \to Z^2$ be iterative dilation (ID) to extend a region. Let $E^i(B): Z^2 \to Z^2$ be iterative erosion (IE) to reduce a region. ID and IE are defined as

$$D^i(B) = \{\cdots((B \oplus SE) \oplus SE)\cdots) \oplus SE\} \quad (4)$$

$$E^i(B) = \{\cdots((B \ominus SE) \ominus SE)\cdots) \ominus SE\} \quad (5)$$

where B is a binary input image, i is a iteration number, $\oplus$ is a dilation operator, and $\ominus$ is an erosion operator. Let, $D^1(B) = D$, $E^1(B) = E$, $D^i(B) = D^i$ and $E^i(B) = E^i$. Let $F(B): Z^2 \to Z^2$ be the 4-connected filling filter.

In order to smooth the boundary, opening and closing filters are used. Let $OP^i(B): Z^2 \to Z^2$ be the iterative opening (IO) filter to smooth thin protrusions. Let $CL^i(B): Z^2 \to Z^2$ be the iterative closing (IC) filter to smooth short gaps. ID and IC are defined as

$$OP^i(B) = \{\cdots((B \circ SE) \circ SE)\cdots) \circ SE\} \quad (6)$$

$$CL^i(B) = \{\cdots((B \cdot SE) \cdot SE)\cdots) \cdot SE\} \quad (7)$$

where B is a binary input image, i is a iteration number, $\circ$ is an opening operator, and $\cdot$ is closing operator. Let $OP^1(B) = OP$, $CL^1(B) = CL$, $OP^i(B) = OP^i$, and $CL^i(B) = CL^i$.

Combination of each filtering has the specific order because the combination order has an influence on the reduction and expansion of the region. Let $CO(B): Z^2 \to Z^2$ be ordered combination function of BM filtering. Used $CO(B)$ in this research is $\{F, E, F, D, CL^{10}, OP^{10}\}$ with SE_2 and SE_3.. Then the binary image obtained by BM filtering is transformed to the gray-level. Let $I_{liver} \subset Z^2$ be a gray-level image. Assuming that B and I have same size, I_{liver} is obtained by pixel by pixel multiplication,

$$I_{liver} = \{(m,n) \mid B(m,n) \otimes I(m,n)\} \quad (8)$$

where B is the binary image and I is the CE-CT image.

Fig. 6 shows the example of BM filtering. The binary image B, is shown in Fig. 6(a). Fig. 6(b) and 6(c) are filling and the binary image after boundary smoothing. Finally, the gray-level liver I_{liver} is created as shown in Fig. 6(d).

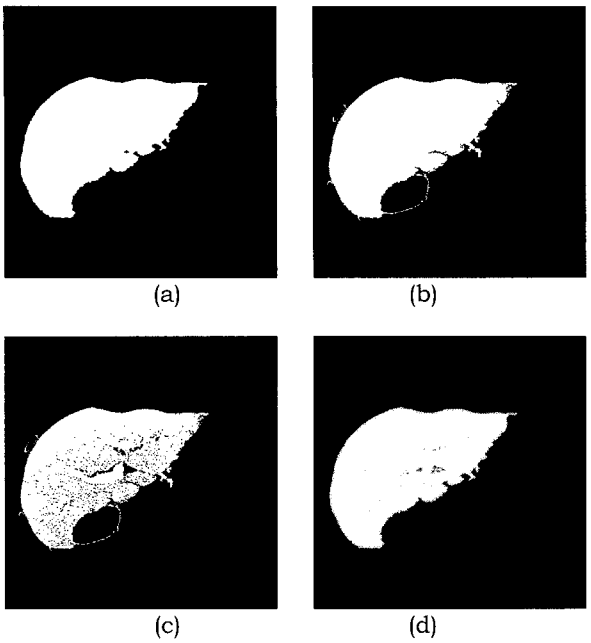

Fig. 6. BM filtering: (a) binary image *B*, (b) filling, (c) binary image after boundary smoothing, and (d) gray-level liver, I_{liver}.

EXPERIMENTS

CT images to be used in this research were provided by Chonnam National University Hospital in Kwangju, Korea. The CT scans were obtained by using a LightSpeed Qx/i, which was produced by GE Medical Systems. Scanning was performed with intravenous contrast enhancement and the CT image was taken at venous phase.

Also, the scanning parameters used a tube current of 230 mAs and 120 kVp, a 30 cm field of view, 5 mm collimation and a table speed of 15 mm/sec (pitch factor, 1:3).

Six patients were selected for testing the new proposed method to segregate a liver structure. CT images of each patient consisted of 10 slices which were hard to segregate the liver in the abdomen. Also, one radiologist took a part in this research in order to segregate the liver structure by the manual method.

In order to evaluate automatically segmented results of improved PHT algorithms, an average normalized area (ANA) and area error rate (AER) were used. ANAs of each patient are averaged and normalized by the image size. As another comparison method, area error rate (AER) is used. The AER is defined as [12]

$$AER = \frac{R_{MSM} \oplus R_{ASM}}{R_{MSM}} \times 100\% \quad (9)$$

where R_{MSM} is the pixel region of the manual segmentation method (MSM), R_{ASM} is the pixel region of the automatic segmentation method (ASM), and $R_{ASM} \oplus R_{MSM}$ is the different pixel region of exclusive-OR operation.

RESULTS AND ANALYSIS

In this section, results of the proposed ASM and MSM drawn by a radiologist were compared. Fig. 6 shows ANA per each patient. The left and right bars are ANAs of the ASM and MSM. As the total ANAs between the ASM and MSM are 0.1569 and 0.1656, the difference is 0.0087. This difference informs strong similarity performance of both methods. Also, Table 1 shows AER per each slice of patients. Average AER is 4.12 ~ 10.65%. As the total average AER is 7.21%, this AER is much improved than previous researchers using semi-automatic segmentation methods [1,12].

Table 1. Area error rate (%).

Patient	1	2	3	4	5	6
Slice 01	9.01	3.31	11.73	13.02	5.82	6.42
Slice 02	6.55	3.45	7.53	9.89	4.88	6.49
Slice 03	4.59	4.17	6.15	11.79	4.24	6.33
Slice 04	4.88	3.41	8.61	11.48	4.38	7.43
Slice 05	4.82	4.35	8.79	9.05	5.85	4.89
Slice 06	5.49	3.59	7.71	9.56	8.56	5.55
Slice 07	6.09	3.54	7.39	7.84	7.91	5.07
Slice 08	4.68	3.99	7.42	11.02	5.61	8.21
Slice 09	7.58	3.95	13.94	9.75	6.59	9.19
Slice 10	5.46	7.41	12.48	13.13	6.81	13.79
Average AER	5.92	4.12	9.18	10.65	6.07	7.34

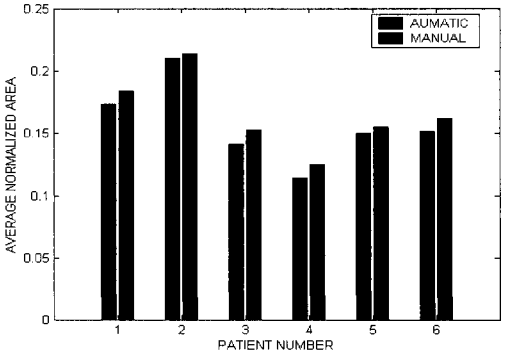

Fig. 7. Average normalized area.

CONCLUSION

In this paper, we proposed an automatic liver segmentation method using improved partial histogram threshold (PHT) algorithms in contrast enhanced CT images. 10 CE-CT slices from six patients (total 60 slices) were selected to evaluate (PHT) algorithms. As the total ANAs between the ASM and MSM were 0.1569 and 0.1656, the difference was 0.0087. Also, the total average AER was 7.21%, From these experimental results, automatic liver segmentation using PHT algorithms and manual segmentation have strong similarity performance. In the future, a three dimensional volume of the liver will be built and hepatic tumor segmentation will be researched.

REFERENCES

[1] K. T. Bae, M. L. Giger, C. T. Chen, and Jr. C. E. Kahn, *"Automatic segmentation of liver structure in CT images"*, Med. Phys., Vol. 20, pp. 71-78, 1993.

[2] L. Gao, D. G. Heath, B. S. Kuszyk, and E. K. Fishman, *"Automatic liver segmentation techn- ique for three-dimensional visualization of CT data"*, Radiology, Vol. 201, pp. 359-364, 1996.

[3] D. Tsai, *"Automatic segmentation of liver struc- ture in CT images using a neural network"*, IEICE Trans. Fundamentals, Vol.E77-A, No. 11, pp. 1892-1895, 1994.

[4] S. A. Husain and E. Shigeru, *"Use of neural networks for feature based recognition of liver region on CT images"*, Neural Networks for Sig. Proc.-Proceedings of the IEEE Work., Vol.2, pp. 831-840, 2000.

[5] K. S. Seo, L. C. Ludeman, S. J. Park, and J. A. Park, *"Efficient liver segmentation based on the spine"*, LNCS 3261, pp. 400-409, 2004.

[6] K. S. Seo, S. J. Park, and J. A. Park, *"Fully automatic liver segmentation based on the morphological property of a CT image"*, Korean J. of Med. Phy., Vol. 15, No. 2, pp. 70-76, 2004.

[7] L. G. Shapiro and G. C. Stockman, Computer Vision, Prentice-Hall, Upper Saddle River, NJ, 2001.

[8] S. J. Orfanidis, Introduction to signal Processing, Prentice Hall. Upper Saddle River, NJ, 1996.

[9] R. J. Schilling and S. L. Harris, Applied Numer- ical Methods for Engineers, Brooks/Cole Publishing Com., Pacific Grove, CA, 2000.

[10] I. Pitas, Digital Image Processing Algorithms and Applications, Wiley & Sons, Inc. New York, NY, 2000.

[11] B. Jahne, Digital Image Processing, 5th., Springer-Verlag, Berlin Heidelberg, 2002.

[12] Sungkee Lee, *"Extraction of the liver from computed tomography using co-occurrence b matrix"*, J. Biomed. Eng. Res., Vol. 22, No.1, pp. 9-17, 2001.